Master equation for collective spontaneous emission with quantized atomic motion

François Damanet,[1] Daniel Braun,[2] and John Martin[1]
[1]*Institut de Physique Nucléaire, Atomique et de Spectroscopie, Université de Liège, Bât. B15, B-4000 Liège, Belgium*
[2]*Institut für theoretische Physik, Universität Tübingen, 72076 Tübingen, Germany*
(Received 24 December 2015; published 26 February 2016)

We derive a Markovian master equation for the internal dynamics of an ensemble of two-level atoms including all effects related to the quantization of their motion. Our equation provides a unifying picture of the consequences of recoil and indistinguishability of atoms beyond the Lamb-Dicke regime on both their dissipative and conservative dynamics, and applies equally well to distinguishable and indistinguishable atoms. We give general expressions for the decay rates and the dipole-dipole shifts for any motional states, and we find closed-form formulas for a number of relevant states (Gaussian states, Fock states, and thermal states). In particular, we show that dipole-dipole interactions and cooperative photon emission can be modulated through the external state of motion.

DOI: 10.1103/PhysRevA.93.022124

I. INTRODUCTION

Spontaneous emission of light from initially excited atoms became one of the corner stones of our understanding of the interaction of light and matter, soon after the introduction of the "photon." It was introduced phenomenologically by Einstein [1] through his famous A-coefficient that gives the rate of spontaneous deexcitation of an excited atom. Later, spontaneous emission was understood through the theory of Wigner and Weisskopf [2] as the result of the perturbation of an atom through the vacuum fluctuations of the electromagnetic field surrounding the atom. The infinitely large number of modes involved in the process leads to effectively irreversible behavior. Once this mechanism was understood, it became clear that the rate with which the excitation of an atom in a given state decays is not a natural constant for this atom, but can be influenced by its environment. By engineering the mode structure of the electromagnetic environment of an atom, in particular through modifying the density of states of the field modes at the resonance frequency, spontaneous emission can be enhanced (in the case of an increased density of states), or reduced (in the opposite case), as first found by Purcell in the context of nuclear resonance [3]. This important insight is now routinely used in photonic crystals, where an electromagnetic band-structure can be designed at will and used for creating e.g. a band gap around the resonance frequency, resulting in largely increased lifetime of an excited atom, inverted spin, exciton, or plasmonic excitation [4–6].

Even earlier, Dicke studied spontaneous emission of several atoms in close vicinity of each other, and found that in such a case spontaneous emission becomes a cooperative effect in which the amplitudes of all atoms emitting simultaneously interfere. Depending on the initial collective internal state of the atoms, emission can be largely enhanced (superradiance), or reduced (subradiance) [7]. Superradiance developed to a large research field in its own right [8–23], culminating recently in matter-wave superradiance in cold atomic gases [24]. It was soon realized that dipole-dipole interactions between atoms can significantly alter these cooperative processes [25–31], but can also be exploited for a variety of purposes, such as the (partial) trapping of light [32] or the implementation of quantum gates using the dipole blockade [33].

In this paper, we reveal yet a third mechanism how spontaneous emission can be influenced: collective emission can be largely "quantum programed" by engineering the external quantum state of motion of the atoms. To this end, we derive a master equation that fully takes into account the quantum nature of the atomic motion and, when relevant, the indistinguishability of atoms. This is essential when the atoms form a Bose-Einstein condensate or are loaded in an optical lattice. For example, when two fermionic atoms are placed in the same potential well and motional state, one in the internal excited state and the other in the ground state, the Pauli exclusion principle forbids the main decay channel, and leads to an increased lifetime of the atomic excited state (see, e.g. [34]). Moreover, it has been known for a long time that the coherence of radiation scattering off atoms in a solid (e.g., in x-ray or neutron scattering) can be influenced through the thermal motion of the atoms. This results in the Debye-Waller factor [35,36] that describes the reduction of visibility of interference maxima as function of temperature. But while in a solid one has in general little influence on the state of motion of the atoms (apart from controlling the temperature of the lattice), a whole new world has opened up in the physics of ion traps and cold atoms. There, the external motional state can now be very well controlled and engineered, to the extent that quantum gates coupling internal states of the atoms originally relied heavily on the use of precise states of this external "quantum bus" [37], even though this requirement could be relaxed later [38].

Thus the quantum nature of the atomic motion appears to be an efficient way to influence the internal dynamics of atoms and its engineering has a wide range of potential applications [39]. However, it turns out that most of the methods used to describe the internal dynamics of atoms including a quantum treatment of their motion are either restricted to the Lamb-Dicke regime [40–46] or do not account for both recoil and indistinguishability [47–52]. Therefore, it appears worthwhile to develop a general theory of spontaneous emission of an ensemble of atoms valid for arbitrary quantum states of motion, which is the purpose of this paper. The master equation we derive constitutes a powerful tool to study the combined effects of the recoil and the indistinguishability of atoms on both their dissipative and conservative internal dynamics, even beyond

the Lamb-Dicke regime. The dependence of the dipole-dipole interactions as well as the lifetime under spontaneous emission on the motional state of the atoms might be observable in dense Rydberg gases, which are under intense current experimental and theoretical investigation [53–56].

The paper is organized as follows. In Sec. II, we present our model. In Sec. III, we derive a general master equation for the internal dynamics of atoms valid for arbitrary motional states. In Sec. IV, we provide general expressions for the dipole-dipole shifts and decay rates which determine the conservative and dissipative part of the master equation, and discuss the effects of the indistinguishability of atoms on these quantities. In Sec. V, we calculate explicitly the decay rates and the dipole-dipole shifts for particularly relevant motional states (Gaussian states, Fock states, and thermal states), both for distinguishable and indistinguishable atoms.

II. MODEL AND HAMILTONIAN

We consider N identical two-level atoms spontaneously emitting photons due to their interaction with the free electromagnetic field initially in vacuum, and treat their motion quantum mechanically. In the point of view of Power-Zienau-Wolley (multipolar coupling scheme [57–59]), the Hamiltonian describing the composite system is

$$H = H_A + H_F + H_{AF}, \tag{1}$$

with H_A the Hamiltonian of the atoms, H_F the Hamiltonian of the free field, and H_{AF} the interaction Hamiltonian responsible for emission or absorption of photons and field-mediated interactions between atoms.

In Eq. (1), the atomic Hamiltonian $H_A = H_A^{\text{ex}} + H_A^{\text{in}} + H_A^{\text{self}}$ consists of an external, an internal, and a self-interaction part, respectively given by

$$H_A^{\text{ex}} = \sum_{j=1}^{N} \left(\frac{\hat{\mathbf{p}}_j^2}{2M} + V(\hat{\mathbf{r}}_j) \right), \tag{2}$$

$$H_A^{\text{in}} = \frac{\hbar\omega_0}{2} \sum_{j=1}^{N} \sigma_z^{(j)}, \tag{3}$$

$$H_A^{\text{self}} = \frac{1}{2\epsilon_0} \int |\hat{\mathbf{P}}(\mathbf{r})|^2 \, d\mathbf{r}. \tag{4}$$

The external part H_A^{ex} corresponds to the kinetic and potential energy of the atoms, with $\hat{\mathbf{r}}_j$ and $\hat{\mathbf{p}}_j$ the center-of-mass position and momentum operators of atom j ($j = 1, \ldots, N$) of mass M and $V(\mathbf{r})$ the external potential experienced by the atoms [60]. We include the spin degree of freedom in the internal state and consider an external potential which does not depend on the spin. This form of H_A^{ex} is quite general and can account for a wide range of experimental settings. The internal part H_A^{in} of the atomic Hamiltonian corresponds to the internal energy of the atoms, with ω_0 the atomic transition frequency and $\sigma_z^{(j)} = |e_j\rangle\langle e_j| - |g_j\rangle\langle g_j|$ with $|g_j\rangle$ ($|e_j\rangle$) the lower (upper) level of atom j of energy $-\hbar\omega_0/2$ ($\hbar\omega_0/2$). Finally, the self-interaction part H_A^{self} corresponds to the self-energy and contact interaction between atoms, with ϵ_0 the permittivity of free space and $\hat{\mathbf{P}}(\mathbf{r})$ the atomic polarization density, given in the dipole approximation by [58]

$$\hat{\mathbf{P}}(\mathbf{r}) = \sum_{j=1}^{N} \mathbf{D}_j \, \delta(\mathbf{r} - \hat{\mathbf{r}}_j), \tag{5}$$

where $\mathbf{D}_j = \mathbf{d}_j \, \sigma_-^{(j)} + \mathbf{d}_j^* \, \sigma_+^{(j)}$ is the dipole operator for atom j, with dipole matrix element $\mathbf{d}_j = \langle g_j|\mathbf{D}_j|e_j\rangle$, $\sigma_-^{(j)} = |g_j\rangle\langle e_j|$, $\sigma_+^{(j)} = |e_j\rangle\langle g_j|$, and δ is the Dirac delta distribution. We consider a polarized atomic sample in which all atoms share the same dipole moment, i.e., $\mathbf{d}_j = \mathbf{d} \; \forall \, j$. The dipole moment $\mathbf{d}$ can be decomposed in the spherical basis $\{\boldsymbol{\varepsilon}_0 \equiv \mathbf{e}_z, \boldsymbol{\varepsilon}_\pm \equiv \mp(\mathbf{e}_x \pm i\mathbf{e}_y)/\sqrt{2}\}$ with $\{\mathbf{e}_x, \mathbf{e}_y, \mathbf{e}_z\}$ the Cartesian unit vectors and the z axis taken as the quantization axis,

$$\mathbf{d} = \sum_{q=0,\pm} d_q \, \boldsymbol{\varepsilon}_q. \tag{6}$$

For a π transition from the upper to the lower level, the only nonvanishing component in (6) is d_0, whereas for a $\sigma^\pm$ transition, the only nonvanishing component is $d_\mp$.

In Eq. (1), the free field Hamiltonian H_F reads

$$H_F = \sum_{\mathbf{k}\boldsymbol{\varepsilon}} \hbar\omega_k \, a_{\mathbf{k}\boldsymbol{\varepsilon}}^\dagger a_{\mathbf{k}\boldsymbol{\varepsilon}}, \tag{7}$$

with $\omega_k = ck$, $k = |\mathbf{k}|$, c the speed of light in vacuum, and $a_{\mathbf{k}\boldsymbol{\varepsilon}}$ ($a_{\mathbf{k}\boldsymbol{\varepsilon}}^\dagger$) the annihilation (creation) operator of a mode of the radiation field of wave vector $\mathbf{k}$ and polarization $\boldsymbol{\varepsilon}$. Note that, in Eq. (7), we have dropped the zero-point energy of the radiation field, as it has no influence on the dynamics of the system.

In the dipole approximation (when the typical size of the atoms is much smaller than the wavelength of the emitted radiation) and the interaction picture with respect to $H_0 \equiv H_A^{\text{ex}} + H_A^{\text{in}} + H_F$, the interaction Hamiltonian $H_{AF}(t)$ reads

$$H_{AF}(t) = -\sum_{j=1}^{N} \mathbf{D}_j(t) \cdot \mathbf{E}(\hat{\mathbf{r}}_j(t), t), \tag{8}$$

with the electric field operator

$$\mathbf{E}(\mathbf{r}, t) = i \sum_{\mathbf{k}\boldsymbol{\varepsilon}} \mathcal{E}_k \, (a_{\mathbf{k}\boldsymbol{\varepsilon}} \, \boldsymbol{\varepsilon}_{\mathbf{k}} \, e^{i(\mathbf{k}\cdot\mathbf{r} - \omega_k t)} - \text{H.c.}), \tag{9}$$

where H.c. stands for Hermitian conjugate, $\mathcal{E}_k = \sqrt{\hbar\omega_k/2\epsilon_0 L^3}$, L^3 is the electromagnetic mode quantization volume, $\boldsymbol{\varepsilon}_{\mathbf{k}}$ the normalized polarization vector, and

$$\hat{\mathbf{r}}_j(t) = e^{iH_A^{\text{ex}} t/\hbar} \, \hat{\mathbf{r}}_j \, e^{-iH_A^{\text{ex}} t/\hbar}. \tag{10}$$

Performing the Schmidt decomposition of the dipole interaction Hamiltonian (8), we get [61]

$$H_{AF}(t) = \sum_{j=1}^{N} \sum_{\omega = \pm\omega_0} e^{-i\omega t} A_j^{\text{in}}(\omega) \otimes B_j(t), \tag{11}$$

with the *quantum jump operators*

$$A_j^{\text{in}}(\pm\omega_0) = \sigma_\mp^{(j)}, \tag{12}$$

and the *bath operators*

$$B_j(t) = -\mathbf{d} \cdot \mathbf{E}(\hat{\mathbf{r}}_j(t), t) \tag{13}$$

defined for any atom $j = 1, \ldots, N$.

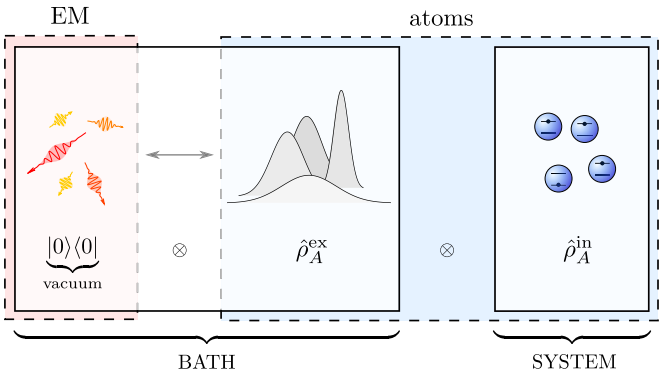

FIG. 1. Decomposition of the global system into bath and system of interest. The system of interest is the internal part of the atoms described by the state $\rho_A^{\rm in}$. The bath corresponds to the atomic external degrees of freedom, described by the state $\rho_A^{\rm ex}$, and the electromagnetic field degrees of freedom, initially in the vacuum state $|0\rangle\langle 0|$.

III. GENERAL MASTER EQUATION FOR THE INTERNAL DYNAMICS

We are interested in the internal dynamics of the atoms only, since our aim is to quantify the effects of the quantization of the atomic motion on cooperative spontaneous emission. In this section, we derive a Markovian master equation for the internal degrees of freedom from a microscopic approach [61]. The derivation of a quantum optical master equation is commonly made for atoms at fixed positions. Here, we go beyond this approximation by treating the atomic position quantum mechanically. The atomic internal degrees of freedom specify our system S, and all other degrees of freedom (atomic external and electromagnetic field degrees of freedom) specify the bath B to which S is coupled, as illustrated in Fig. 1. Since the master equation we obtain takes the usual standard form, we only present here the key steps of the derivation [62]. The detailed calculations can be found in the Supplemental Material [63].

A. Microscopic derivation and general form of the master equation

Our starting point is the Liouville–von Neumann evolution equation

$$i\hbar\frac{d\rho(t)}{dt} = \left[H_A^{\rm self}(t) + H_{AF}(t), \rho(t)\right] \tag{14}$$

for the global density matrix $\rho(t)$ in the interaction picture with respect to H_0. The master equation for the internal atomic dynamics only is obtained by tracing over the bath degrees of freedom and by performing the Born-Markov approximation we justify below.

1. Born-Markov approximation and correlation functions

In the weak coupling regime, the Born approximation (see, e.g. [61]) assumes the form

$$\rho(t) \approx \rho_A^{\rm in}(t) \otimes \rho_B, \tag{15}$$

for the global density matrix. Here $\rho_A^{\rm in}(t) = {\rm Tr}_B[\rho(t)]$ is the reduced density matrix of S (in the interaction picture) describing the atomic internal dynamics, where ${\rm Tr}_B[\,\cdot\,]$ denotes the trace over the bath degrees of freedom. The bath is described by $\rho_B = \rho_A^{\rm ex} \otimes \rho_F$, where $\rho_A^{\rm ex}$ is the motional density matrix and where $\rho_F = |0\rangle\langle 0|$ is the electromagnetic field density matrix which we take as the vacuum state [64]. The Born approximation excludes correlations between external and internal states. In this approximation, the bath is considered as stationary during the whole relaxation dynamics and the influence of the system on the bath is neglected. Accordingly, we consider in this work that the characteristic evolution time τ_M of the atomic motion is much larger than the relaxation time τ_R of the system. This condition is met in a wide range of experimental situations where atoms are optically or magnetically trapped. For example, the typical frequency Ω_M of a harmonic potential produced with visible light is in the range 1–10^3 Hz, which leads to $\tau_M \sim 1/\Omega_M \gg \tau_R \sim 1/\gamma_0$ where γ_0 is the single-atom free spontaneous emission rate, of the order of 10^9 Hz for optical transitions (i.e., there are at least six orders of magnitude separation between τ_M and τ_R). Therefore, the atomic motion is approximately frozen during the emission of photons, so that $\hat{\mathbf{r}}_j(t) \approx \hat{\mathbf{r}}_j(0) = \hat{\mathbf{r}}_j$.

The Markov approximation which eliminates memory effects is justified as long as the bath correlation time τ_B is much smaller than the typical relaxation time τ_R of the system. It is well established that the Markov approximation is an excellent approximation for describing the process of spontaneous emission of photons from atoms at fixed positions [65]. We now show that this is also the case when the bath operators B_j [Eq. (13)] contain in addition the motional degrees of freedom. The relevant correlation function $\mathcal{C}_{ij}(t)$ that determines the correlation time τ_B is [61]

$$\mathcal{C}_{ij}(t) = \langle B_i^\dagger(t) B_j(0)\rangle_B, \tag{16}$$

where $B_j(t)$ is given by Eq. (13) and the expectation value is over the bath degrees of freedom. Explicitly, for $\hat{\mathbf{r}}_j(t) \approx \hat{\mathbf{r}}_j$, the correlation function reads

$$\mathcal{C}_{ij}(t) \approx \frac{1}{L^3}\sum_{\mathbf{k}\boldsymbol{\varepsilon}} \mathcal{C}_{\mathbf{k}\boldsymbol{\varepsilon}}^{\rm em}(t)\, \mathcal{C}_{ij}^{\rm ex}(\mathbf{k}), \tag{17}$$

with

$$\mathcal{C}_{\mathbf{k}\boldsymbol{\varepsilon}}^{\rm em}(t) = \frac{\hbar\omega_k}{2\epsilon_0}\,|\boldsymbol{\varepsilon}_{\mathbf{k}}\cdot\mathbf{d}|^2\, e^{-i\omega_k t} \tag{18}$$

and the motional correlation function

$$\mathcal{C}_{ij}^{\rm ex}(\mathbf{k}) = \langle e^{i\mathbf{k}\cdot\hat{\mathbf{r}}_{ij}}\rangle_{\rm ex} = {\rm Tr}_{ij}\left[e^{i\mathbf{k}\cdot\hat{\mathbf{r}}_{ij}}\rho_{ij}^{\rm ex}\right], \tag{19}$$

where $\hat{\mathbf{r}}_{ij} = \hat{\mathbf{r}}_i - \hat{\mathbf{r}}_j$ and where the trace is now performed over the motional degrees of freedom of the atoms i and j with $\rho_{ij}^{\rm ex}$ their external reduced density matrix.

For atoms at fixed classical positions, which is obtained formally through the substitution $\hat{\mathbf{r}}_i \to \mathbf{r}_i$, the motional correlation function (19) reduces to $\mathcal{C}_{ij}^{\rm ex}(\mathbf{k}) = e^{i\mathbf{k}\cdot\mathbf{r}_{ij}}$ with $\mathbf{r}_{ij} = \mathbf{r}_i - \mathbf{r}_j$ the vector connecting atoms i and j, so that Eq. (18) yields the Fourier components of the classical correlation function for the electromagnetic field. The bath correlation time τ_B is smaller than an optical period, and thereby much smaller than the spontaneous emission time τ_R and justifies the

Markov approximation. When the atomic motion is quantized, the plane waves $e^{i\mathbf{k}\cdot\mathbf{r}_{ij}}$ in the Fourier series (17) are replaced by $\langle e^{i\mathbf{k}\cdot\hat{\mathbf{r}}_{ij}}\rangle_{\rm ex}$ to account for the fluctuations and correlations in the positions of atoms i and j. However, since the electric field correlations decay on a time scale τ_B regardless of the positions, we see that the motion of the atoms does not increase the bath correlation time, and the Markov approximation remains therefore justified.

2. *Standard form of the master equation*

Under the Born-Markov approximation justified above and the usual rotating wave approximation [66], we get the following standard form of the master equation for the reduced density matrix $\rho_A^{\rm in}(t)$ describing the internal atomic dynamics only:

$$\frac{d\rho_A^{\rm in}(t)}{dt} = -\frac{i}{\hbar}\big[H_\Omega + \langle H_A^{\rm self}\rangle_{\rm ex}, \rho_A^{\rm in}(t)\big] + \mathcal{D}\big(\rho_A^{\rm in}(t)\big), \quad (20)$$

with the level-shift Hamiltonian

$$H_\Omega = \sum_{i,j=1}^{N} \hbar\Omega_{ij}\, \sigma_+^{(i)}\sigma_-^{(j)} \quad (21)$$

in terms of level shifts

$$\Omega_{ij} = \mathrm{Im}[\Gamma_{ij}(\omega_0) + \Gamma_{ij}(-\omega_0)], \quad (22)$$

and the dissipator

$$\mathcal{D}(\cdot) = \sum_{i,j=1}^{N} \gamma_{ij}\left(\sigma_-^{(j)}\cdot\sigma_+^{(i)} - \frac{1}{2}\{\sigma_+^{(i)}\sigma_-^{(j)},\cdot\}\right) \quad (23)$$

in terms of decay rates

$$\gamma_{ij} = 2\,\mathrm{Re}[\Gamma_{ij}(\omega_0)]. \quad (24)$$

The spectral correlation tensor Γ_{ij} which determines the level shifts and the decay rates is defined as

$$\Gamma_{ij}(\omega) = \frac{1}{\hbar^2}\int_0^\infty e^{i\omega t}\, \mathcal{C}_{ij}(t)\, dt, \quad (25)$$

where $\mathcal{C}_{ij}(t)$ is the correlation function given by Eq. (17). Note that in Eq. (20), $\langle H_A^{\rm self}\rangle_{\rm ex}$ stands for the expectation value of $H_A^{\rm self}$ over the atomic external degrees of freedom and does not depend anymore on time because of the approximation $\hat{\mathbf{r}}_j(t) \approx \hat{\mathbf{r}}_j$. Figure 2 summarizes all the approximations performed in the derivation of the master equation (20) in terms of the relevant characteristic time scales.

Equations (21) and (23) describe respectively the conservative and dissipative dynamics of the atomic internal state caused by the interaction with the electromagnetic field. The level shifts Ω_{ij} and the decay rates γ_{ij} are obtained from the imaginary and real parts of the spectral correlation tensor Γ_{ij} [Eq. (25)]. In the following, we analyze more precisely the structure of these coefficients entering the master equation.

B. Dissipative part

An explicit expression for the decay rates γ_{ij} [Eq. (24)] can be obtained by performing the time integration in Eq. (25) together with Eq. (17) for the bath correlation function, thereby

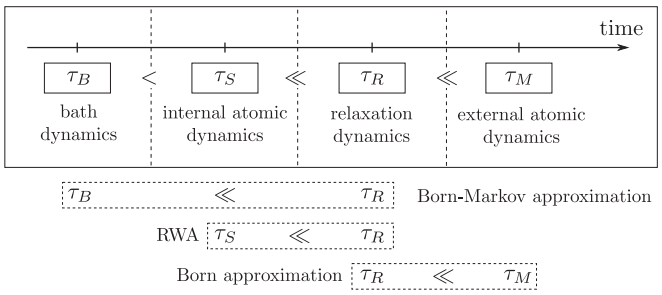

FIG. 2. Characteristic time scales corresponding to the evolution of the external dynamics (τ_M), the internal dynamics ($\tau_R \sim 1/\gamma_0$ with γ_0 the free spontaneous emission rate), the isolated system dynamics ($\tau_S \sim 1/\omega_0$ with ω_0 the atomic transition frequency), and the bath ($\tau_B < \tau_S$).

yielding

$$\gamma_{ij} = \frac{1}{L^3}\sum_{\mathbf{k}\boldsymbol{\varepsilon}} \gamma_{\mathbf{k}\boldsymbol{\varepsilon}}^{\rm em}\, \mathcal{C}_{ij}^{\rm ex}(\mathbf{k}), \quad (26)$$

with

$$\gamma_{\mathbf{k}\boldsymbol{\varepsilon}}^{\rm em} = \frac{\pi\omega_k}{\hbar\epsilon_0}\,|\boldsymbol{\varepsilon}_\mathbf{k}\cdot\mathbf{d}|^2\,\delta(\omega_k - \omega_0) \quad (27)$$

the Fourier components of the decay rates for classical atomic positions. Equation (26) shows that the Fourier components of the decay rates are affected by the quantization of the atomic motion through weighting by the motional correlation function (19). In the limit of a continuum of modes, the sum over the wave vectors can be replaced by an integral [we use the standard spherical coordinates (k,θ,φ) with $d\Omega = \sin\theta\, d\theta\, d\varphi$],

$$\frac{1}{L^3}\sum_{\mathbf{k}} \to \int \frac{d\mathbf{k}}{(2\pi)^3} \equiv \frac{1}{(2\pi)^3 c^3}\int_0^{+\infty} \omega^2\, d\omega \int d\Omega, \quad (28)$$

and Eq. (26) yields, after performing the ω-integration,

$$\gamma_{ij} = \int \sum_{\boldsymbol{\varepsilon}} \gamma_{\mathbf{k}_0\boldsymbol{\varepsilon}}^{\rm em}\, \mathcal{C}_{ij}^{\rm ex}(\mathbf{k}_0)\, \frac{d\Omega}{(2\pi)^2}, \quad (29)$$

with $\mathbf{k}_0 = k_0\,(\cos\varphi\sin\theta, \sin\varphi\sin\theta, \cos\theta)$, $k_0 = \omega_0/c$,

$$\gamma_{\mathbf{k}_0\boldsymbol{\varepsilon}}^{\rm em} = \frac{3\pi\gamma_0}{2}|\boldsymbol{\varepsilon}_{\mathbf{k}_0}\cdot\mathbf{e}_\mathbf{d}|^2, \quad (30)$$

with $\mathbf{e}_\mathbf{d} = \mathbf{d}/d$, $d = |\mathbf{d}|$, and γ_0 the single-atom spontaneous emission rate

$$\gamma_0 = \frac{\omega_0^3 d^2}{3\pi\hbar\epsilon_0 c^3}. \quad (31)$$

For classical atomic positions, $\mathcal{C}_{ij}^{\rm ex}(\mathbf{k}) = e^{i\mathbf{k}\cdot\mathbf{r}_{ij}}$ and Eq. (29) reduces to the classical form of the decay rates for atoms separated by a distance $r_{ij} = |\mathbf{r}_{ij}|$, $\gamma_{ij} = \gamma^{\rm cl}(\mathbf{r}_{ij})$ with [67,68]

$$\gamma^{\rm cl}(\mathbf{r}_{ij}) = \frac{3\gamma_0}{2}\left[p_{ij}\,\frac{\sin\xi_{ij}}{\xi_{ij}} + q_{ij}\left(\frac{\cos\xi_{ij}}{\xi_{ij}^2} - \frac{\sin\xi_{ij}}{\xi_{ij}^3}\right)\right], \quad (32)$$

with $\xi_{ij} = k_0 r_{ij}$. For a π transition, the angular factors p_{ij} and q_{ij} are given by

$$p_{ij} = \sin^2\alpha_{ij}, \quad q_{ij} = (1 - 3\cos^2\alpha_{ij}), \quad (33)$$

and for a $\sigma^{\pm}$ transition by

$$p_{ij} = \tfrac{1}{2}(1+\cos^2\alpha_{ij}), \quad q_{ij} = \tfrac{1}{2}(3\cos^2\alpha_{ij}-1), \tag{34}$$

with $\alpha_{ij} = \arccos(\mathbf{r}_{ij}\cdot\mathbf{e}_z/r_{ij})$ the angle between the quantization axis and the vector connecting atoms i and j. Equation (29) can also be written as $\gamma_{ij} = \mathcal{F}_{\mathbf{0}}^{-1}[\mathcal{F}_{\mathbf{k}}[\gamma^{\rm cl}]\mathcal{C}_{ij}^{\rm ex}(\mathbf{k})]$ which can be seen to be the convolution product $(\gamma^{\rm cl} \star f_{ij})(\mathbf{0})$ with $f_{ij}(\mathbf{r}) = \mathcal{F}_{\mathbf{r}}^{-1}[\mathcal{C}_{ij}^{\rm ex}(\mathbf{k})]$ [69]. Therefore, the decay rates takes the alternative form

$$\gamma_{ij} = \int_{\mathbb{R}^3} \gamma^{\rm cl}(\mathbf{r})\, \mathcal{F}_{\mathbf{r}}^{-1}\big[\mathcal{C}_{ij}^{\rm ex}(\mathbf{k})\big] d\mathbf{r} \tag{35}$$

in terms of their classical expression (32) and the inverse Fourier transform of the motional correlation function (19).

Two important features follow from Eq. (29) [or equivalently from Eq. (35)]. First, the diagonal decay rates γ_{ii} are seen to coincide with those obtained in the classical case because $\mathcal{C}_{ii}^{\rm ex}(\mathbf{k}) = 1$ for any motional state and wave vector $\mathbf{k}$. Hence the dissipative internal dynamics of a single atom is not affected by its motional state when the electromagnetic field is initially in vacuum. Second, Eq. (29) shows that as soon as the quantum nature of the atomic motion becomes appreciable, we have the additional possibility of influencing the decay rates through engineering the motional state of the atoms. The motional correlation function $\mathcal{C}_{ij}^{\rm ex}(\mathbf{k}_0)$ can be seen from Eq. (29) to play a similar role as mode-dependent modifications of the coupling constants, and can thus be expected to lead to similar effects as Purcell's enhancement or reduction of spontaneous emission [34].

It readily follows from Eq. (35) that $\gamma_{ij} = \gamma_{ji}$ and $|\gamma_{ij}| \leqslant \gamma_0$. Indeed, the classical expression (32) satisfies $|\gamma^{\rm cl}(\mathbf{r})| \leqslant \gamma^{\rm cl}(\mathbf{0}) = \gamma_0\ \forall\,\mathbf{r}$, which implies

$$|\gamma_{ij}| \leqslant \gamma_0 \left| \int_{\mathbb{R}^3} \mathcal{F}_{\mathbf{r}}^{-1}\big[\mathcal{C}_{ij}^{\rm ex}(\mathbf{k})\big] d\mathbf{r} \right| = \gamma_0 \big|\mathcal{C}_{ij}^{\rm ex}(\mathbf{0})\big| = \gamma_0 \tag{36}$$

since $\mathcal{C}_{ij}^{\rm ex}(\mathbf{0}) = \mathrm{Tr}(\rho_{ij}^{\rm ex}) = 1$ for any i,j due to normalization.

C. Conservative part

An explicit expression for the level shifts Ω_{ij} [Eq. (22)] can be obtained along the same lines as for the decay rates, and reads

$$\Omega_{ij} = \frac{1}{L^3} \sum_{\mathbf{k}\boldsymbol{\varepsilon}} \Omega_{\mathbf{k}\boldsymbol{\varepsilon}}^{\rm em}\, \mathcal{C}_{ij}^{\rm ex}(\mathbf{k}), \tag{37}$$

with

$$\Omega_{\mathbf{k}\boldsymbol{\varepsilon}}^{\rm em} = -\frac{1}{\hbar\epsilon_0}\, \mathrm{P}\!\left(\frac{\omega_k^2}{\omega_k^2-\omega_0^2}\right) |\boldsymbol{\varepsilon}_{\mathbf{k}}\cdot\mathbf{d}|^2, \tag{38}$$

where P stands for the Cauchy principal value [70]. In the limit of a continuum of modes, Eq. (37) becomes

$$\Omega_{ij} = \mathrm{P}\int \sum_{\boldsymbol{\varepsilon}} \Omega_{\mathbf{k}\boldsymbol{\varepsilon}}^{\rm em}\, \mathcal{C}_{ij}^{\rm ex}(\mathbf{k})\, \frac{d\mathbf{k}}{(2\pi)^3}, \tag{39}$$

with

$$\Omega_{\mathbf{k}\boldsymbol{\varepsilon}}^{\rm em} = -\frac{3\pi\gamma_0}{k_0^3}\, \frac{k^2}{k^2-k_0^2}\, |\boldsymbol{\varepsilon}_{\mathbf{k}}\cdot\mathbf{d}|^2. \tag{40}$$

As for the decay rates, the plane waves $e^{i\mathbf{k}\cdot\mathbf{r}_{ij}}$ in the Fourier series for the level shifts Ω_{ij} are replaced by the motional correlation function (19) taking into account the quantization of the atomic motion. The diagonal coefficients Ω_{ii} related to the Lamb shifts are not affected by the quantization of the motion since $\mathcal{C}_{ii}^{\rm ex}(\mathbf{k}) = 1$; they are all equal and can be discarded by means of a renormalization of the atomic transition frequency ω_0. The off-diagonal shifts Ω_{ij} $(i \neq j)$ contain divergent contact terms, that are already present without quantization of the atomic motion, i.e., with classical atomic positions. However, these terms are exactly canceled by other divergent terms appearing in the Hamiltonian $H_A^{\rm self}$ [68]. This cancellation still holds when the atomic motion is quantized, as we proceed to show. By keeping only the energy conserving terms (RWA) in Eq. (4), the expectation value $\langle H_A^{\rm self}\rangle_{\rm ex}$ appearing in Eq. (20) becomes

$$\big\langle H_A^{\rm self}\big\rangle_{\rm ex} = \sum_{i\neq j}^{N} \hbar\Omega_{ij}^{\rm self}\sigma_+^{(i)}\sigma_-^{(j)} + \sum_{i=1}^{N} \hbar\Omega_{ii}^{\rm self}\,\mathbb{1}^{(i)}, \tag{41}$$

with $\mathbb{1}^{(i)}$ the internal identity operator for atom i and

$$\Omega_{ij}^{\rm self} = \frac{3\pi\gamma_0}{k_0^3}\int \mathcal{C}_{ij}^{\rm ex}(\mathbf{k})\, \frac{d\mathbf{k}}{(2\pi)^3}, \tag{42}$$

$$\Omega_{ii}^{\rm self} = \frac{3\pi\gamma_0}{2k_0^3}\int \frac{d\mathbf{k}}{(2\pi)^3}. \tag{43}$$

Since the divergent level shift $\Omega_{ii}^{\rm self}$ in Eq. (41) is proportional to the identity, it can be absorbed by means of a redefinition of the zero energy, so that $\langle H_A^{\rm self}\rangle_{\rm ex}$ reduces to

$$\big\langle H_A^{\rm self}\big\rangle_{\rm ex} = \sum_{i\neq j}^{N} \hbar\Omega_{ij}^{\rm self}\sigma_+^{(i)}\sigma_-^{(j)}. \tag{44}$$

We now split the level shifts Ω_{ij} [Eq. (39)] into [68]

$$\Omega_{ij} = \Delta_{ij} - \Omega_{ij}^{\rm self}, \tag{45}$$

where $\Omega_{ij}^{\rm self}$ is given by Eq. (42) and Δ_{ij} is the dipole-dipole shift given by

$$\Delta_{ij} = \mathrm{P}\int \sum_{\boldsymbol{\varepsilon}} \Delta_{\mathbf{k}\boldsymbol{\varepsilon}}^{\rm em}\, \mathcal{C}_{ij}^{\rm ex}(\mathbf{k})\, \frac{d\mathbf{k}}{(2\pi)^3}, \tag{46}$$

with

$$\Delta_{\mathbf{k}\boldsymbol{\varepsilon}}^{\rm em} = \frac{3\pi\gamma_0}{k_0^3}\left[1 - \frac{k^2}{k^2-k_0^2}|\boldsymbol{\varepsilon}_{\mathbf{k}}\cdot\mathbf{e}_{\mathbf{d}}|^2\right]. \tag{47}$$

The Hamiltonian (21) entering the master equation can then be decomposed as

$$H_\Omega = \sum_{i\neq j}^{N} \hbar\Omega_{ij}\,\sigma_+^{(i)}\sigma_-^{(j)} \equiv H_\Delta - \big\langle H_A^{\rm self}\big\rangle_{\rm ex}, \tag{48}$$

with the dipole-dipole Hamiltonian

$$H_\Delta = \sum_{i\neq j}^{N} \hbar\Delta_{ij}\,\sigma_+^{(i)}\sigma_-^{(j)}, \tag{49}$$

so that Eq. (20) eventually reads

$$\frac{d\rho_A^{\rm in}(t)}{dt} = -\frac{i}{\hbar}\big[H_\Delta, \rho_A^{\rm in}(t)\big] + \mathcal{D}\big(\rho_A^{\rm in}(t)\big). \tag{50}$$

Hence $H_A^{\rm self}$ does not contribute to the dynamics, and H_Δ is the proper form of the Hamiltonian to describe the conservative dynamics of the atomic system. It accounts for second-order photon exchanges between pairs of atoms in different internal energy eigenstates [72].

For classical atomic positions, $\mathcal{C}_{ij}^{\rm ex}(\mathbf{k}) = e^{i\mathbf{k}\cdot\mathbf{r}_{ij}}$ and Eq. (46) reduces to the retarded interaction energy (divided by $\hbar$) between two parallel dipoles located at fixed positions $\mathbf{r}_i$ and $\mathbf{r}_j$, i.e., $\Delta_{ij} = \Delta^{\rm cl}(\mathbf{r}_{ij})$ with [67,68]

$$\Delta^{\rm cl}(\mathbf{r}_{ij}) = \frac{3\gamma_0}{4}\left[- p_{ij}\,\frac{\cos\xi_{ij}}{\xi_{ij}} + q_{ij}\left(\frac{\sin\xi_{ij}}{\xi_{ij}^2} + \frac{\cos\xi_{ij}}{\xi_{ij}^3}\right)\right], \tag{51}$$

$\xi_{ij} = k_0 r_{ij}$ and where p_{ij} and q_{ij} are given by Eq. (33) for a π transition, and by Eq. (34) for a $\sigma^\pm$ transition. The sum over the polarizations of the Fourier components (47) is thus equal to the Fourier transform of the retarded dipole-dipole interaction energy (divided by $\hbar$), $\Delta^{\rm cl}(\mathbf{r})$. Equation (46) is the generalization of the dipole-dipole shifts (51) to account for quantum fluctuations and correlations in the atomic motion. Similar to the decay rates, the dipole-dipole shifts can be written as

$$\Delta_{ij} = \int_{\mathbb{R}^3} \Delta^{\rm cl}(\mathbf{r})\,\mathcal{F}_{\mathbf{r}}^{-1}\left[\mathcal{C}_{ij}^{\rm ex}(\mathbf{k})\right] d\mathbf{r}. \tag{52}$$

As an example, let us consider again the case of two atoms at classical positions $\mathbf{r}_i$ and $\mathbf{r}_j$. We then have $\mathcal{C}_{ij}^{\rm ex}(\mathbf{k}) = e^{i\mathbf{k}\cdot\mathbf{r}_{ij}}$ and Eq. (52) reduces to $\Delta_{ij} = \Delta^{\rm cl}(\mathbf{r}_{ij})$, as expected. However, in most cases, Eq. (52) yields an infinite result because the $1/r^3$ divergence of $\Delta^{\rm cl}(\mathbf{r})$ at $r = 0$ is not integrable in $\mathbb{R}^3$ and because $\mathcal{F}_{\mathbf{r}}^{-1}[\mathcal{C}_{ij}^{\rm ex}(\mathbf{k})]$ does in general not vanish at the origin. In order to treat dipole-dipole interactions, one must introduce a minimal distance, i.e., a cutoff, in the integral (52). A natural cutoff would be of the order of the size of an atom, so as to remain compatible with the dipole approximation made in the derivation of the master equation. The effect of the cutoff will be discussed in detail in the following sections.

IV. GENERAL EXPRESSIONS OF DECAY RATES AND DIPOLE-DIPOLE SHIFTS

The master equation (50) is completely determined in terms of the motional correlation function (19) through the expressions of the decay rates γ_{ij}, given by Eq. (35) and appearing in the dissipator (23), and the dipole-dipole shifts Δ_{ij}, given by Eq. (52) and appearing in the dipole-dipole Hamiltonian (49). All the effects related to recoil, quantum fluctuations of motion and indistinguishability are included in the motional correlation function $\mathcal{C}_{ij}^{\rm ex}(\mathbf{k})$. In this section, we provide general expressions for $\mathcal{C}_{ij}^{\rm ex}(\mathbf{k})$, γ_{ij}, and Δ_{ij} both for distinguishable and indistinguishable atoms for arbitrary motional states.

A. Distinguishable atoms

When N distinguishable atoms are in the motional separable state $|\phi_{1_\ell}\dots\phi_{N_\ell}\rangle$ with a probability $p_\ell \geqslant 0$ ($\sum_\ell p_\ell = 1$), the global motional state is the statistical mixture

$$\rho_A^{\rm ex,sep} = \sum_{\ell=1}^{L} p_\ell\,|\phi_{1_\ell}\dots\phi_{N_\ell}\rangle\langle\phi_{1_\ell}\dots\phi_{N_\ell}|. \tag{53}$$

The single-atom motional states $|\phi_{j_\ell}\rangle$ ($j = 1,\dots,N$; $\ell = 1,\dots,L$) are normalized but are not necessarily orthogonal. The two-atom reduced density matrix $\rho_{ij}^{\rm ex}$ is obtained by tracing over the motional degrees of freedom of all atoms but i and j, and reads

$$\rho_{ij}^{\rm ex,sep} = \sum_{\ell=1}^{L} p_\ell\,|\phi_{i_\ell}\phi_{j_\ell}\rangle\langle\phi_{i_\ell}\phi_{j_\ell}|. \tag{54}$$

The motional correlation function (19) is thus given, for distinguishable atoms [in the mixture (53)], by

$$\mathcal{C}_{ij}^{\rm ex,sep}(\mathbf{k}) = \sum_{\ell=1}^{L} p_\ell\, I_{i_\ell i_\ell}(\mathbf{k}) I_{j_\ell j_\ell}(-\mathbf{k}) \tag{55}$$

with the overlap integral

$$\begin{aligned} I_{\alpha\beta}(\mathbf{k}) &= \int_{\mathbb{R}^3} e^{i\mathbf{k}\cdot\mathbf{r}}\,\phi_\alpha(\mathbf{r})\,\phi_\beta^*(\mathbf{r})\,d\mathbf{r} \\ &= \int_{\mathbb{R}^3} \mathcal{F}_{\mathbf{k}'-\mathbf{k}}[\phi_\alpha]\,\mathcal{F}_{\mathbf{k}'}[\phi_\beta^*]\,d\mathbf{k}' \end{aligned} \tag{56}$$

defined for any pair of indices $\alpha\beta$. The overlap integral (56) is equal to the overlap in momentum space between the state ϕ_β and the state ϕ_α shifted by the momentum $\hbar\mathbf{k}$ of a photon of wave vector $\mathbf{k}$. The inverse Fourier transform of (55) can be written

$$\mathcal{F}_{\mathbf{r}}^{-1}\left[\mathcal{C}_{ij}^{\rm ex}(\mathbf{k})\right] = \sum_{\ell=1}^{L} p_\ell \int_{\mathbb{R}^3} |\phi_{i_\ell}(\mathbf{r}')|^2\,|\phi_{j_\ell}(\mathbf{r}+\mathbf{r}')|^2\,d\mathbf{r}'. \tag{57}$$

On inserting Eq. (57) into Eqs. (35) and (52), we obtain explicit expressions for the decay rates and the dipole-dipole shifts in terms of single-atom motional states

$$\gamma_{ij}^{\rm sep} = \sum_{\ell=1}^{L} p_\ell \iint_{\mathbb{R}^3\times\mathbb{R}^3} \gamma^{\rm cl}(\mathbf{r}-\mathbf{r}')\,|\phi_i(\mathbf{r})|^2\,|\phi_j(\mathbf{r}')|^2\,d\mathbf{r}\,d\mathbf{r}', \tag{58}$$

$$\Delta_{ij}^{\rm sep} = \sum_{\ell=1}^{L} p_\ell \iint_{\mathbb{R}^3\times\mathbb{R}^3} \Delta^{\rm cl}(\mathbf{r}-\mathbf{r}')\,|\phi_i(\mathbf{r})|^2\,|\phi_j(\mathbf{r}')|^2\,d\mathbf{r}\,d\mathbf{r}'. \tag{59}$$

B. Indistinguishable atoms

For indistinguishable atoms in a statistical mixture ρ_A, each wave function of the mixture has to be either symmetric or antisymmetric under exchange of particles, depending on the quantum statistics of the atoms (bosonic or fermionic). Due to the Born approximation, the mixture contains a single term and the initial state has to be of the form $\rho_A(0) = \rho_A^{\rm in} \otimes \rho_A^{\rm ex}$. For clarity, we shall consider *pure* product initial states, and restrict ourselves to states that are both individually either symmetric (+) or antisymmetric (−). The symmetrization (antisymmetrization) of the separable motional state $|\phi_1\dots\phi_N\rangle$

leads to the N-atom symmetric (antisymmetric) state

$$\left|\Phi_A^{\mathrm{ex},\pm}\right\rangle = \sqrt{\frac{n_{\phi_1}!\cdots n_{\phi_N}!}{N!}} \sum_{\pi} s_{\pm}^{\pi} \left|\phi_{\pi(1)}\cdots\phi_{\pi(N)}\right\rangle, \tag{60}$$

where n_{ϕ_j} is the number of atoms occupying the single-atom motional state $|\phi_j\rangle$, the sum runs over all permutations π of the indices $\{1,\ldots,N\}$, and the symbol $s_{\pm}^{\pi}$ is defined as

$$s_{\pm}^{\pi} = \begin{cases} 1 & \text{if} + , \\ \mathrm{sign}(\pi) & \text{if} - , \end{cases} \tag{61}$$

where $\mathrm{sign}(\pi)$ is the signature of the permutation π. The two-atom reduced density matrix, obtained by taking the partial trace of $\rho_A^{\mathrm{ex},\pm} = |\Phi_A^{\mathrm{ex},\pm}\rangle\langle\Phi_A^{\mathrm{ex},\pm}|$ over all atoms but i and j, has the form

$$\rho_{ij}^{\mathrm{ex},\pm} = \sum_{\pi,\pi'} \lambda_{ij}^{\pi\pi',\pm} \left|\phi_{\pi(i)}\phi_{\pi(j)}\right\rangle\left\langle\phi_{\pi'(i)}\phi_{\pi'(j)}\right|, \tag{62}$$

with

$$\lambda_{ij}^{\pi\pi',\pm} = \frac{s_{\pm}^{\pi}\, s_{\pm}^{\pi'} \prod_{\substack{n=1 \\ n\neq i,j}}^{N} \langle\phi_{\pi'(n)}|\phi_{\pi(n)}\rangle}{\sum_{\tilde{\pi},\tilde{\pi}'} s_{\pm}^{\tilde{\pi}}\, s_{\pm}^{\tilde{\pi}'} \prod_{n=1}^{N} \langle\phi_{\tilde{\pi}'(n)}|\phi_{\tilde{\pi}(n)}\rangle}. \tag{63}$$

Inserting Eq. (62) into (19) eventually leads to the motional correlation function

$$\mathcal{C}_{ij}^{\mathrm{ex},\pm}(\mathbf{k}) = \sum_{\pi,\pi'} \lambda_{ij}^{\pi\pi',\pm}\, I_{\pi(i)\pi'(i)}(\mathbf{k})\, I_{\pi(j)\pi'(j)}(-\mathbf{k}). \tag{64}$$

An important result is that $\mathcal{C}_{ij}^{\mathrm{ex},\pm}$, and thus γ_{ij} and Δ_{ij} [see Eqs. (29) and (52)], do not depend on i and j for indistinguishable atoms, regardless of the average distance between atoms. This fact has far reaching consequences on how the atomic system radiates, especially in the regime in which cooperative processes are enhanced, when atoms are located within a volume smaller than λ_0^3. For distinguishable atoms, cooperative emission (superradiance or subradiance) is strongly altered by the dephasing of the atomic dipoles as a consequence of dipole-dipole interactions, whereas for indistinguishable atoms no such dephasing occurs.

The reduced density matrix (62) leads to decay rates and dipole-dipole shifts in terms of the following *exchange integrals*

$$\gamma_{ij} = \sum_{\pi,\pi'} \lambda_{ij}^{\pi\pi',\pm} \iint_{\mathbb{R}^3\times\mathbb{R}^3} \gamma^{\mathrm{cl}}(\mathbf{r}-\mathbf{r}')\, \phi_{\pi(i)}(\mathbf{r})\phi_{\pi'(i)}^*(\mathbf{r}) \times \phi_{\pi(j)}(\mathbf{r}')\phi_{\pi'(j)}^*(\mathbf{r}')\, d\mathbf{r}\, d\mathbf{r}', \tag{65}$$

$$\Delta_{ij} = \sum_{\pi,\pi'} \lambda_{ij}^{\pi\pi',\pm} \iint_{\mathbb{R}^3\times\mathbb{R}^3} \Delta^{\mathrm{cl}}(\mathbf{r}-\mathbf{r}')\, \phi_{\pi(i)}(\mathbf{r})\phi_{\pi'(i)}^*(\mathbf{r}) \times \phi_{\pi(j)}(\mathbf{r}')\phi_{\pi'(j)}^*(\mathbf{r}')\, d\mathbf{r}\, d\mathbf{r}'. \tag{66}$$

A particularly relevant situation in the context of cold-atom physics is when all atoms occupy the same motional state $|\phi_0\rangle$ and thus form a Bose-Einstein condensate, i.e., when the global motional state $\rho_A^{\mathrm{ex}} = (|\phi_0\rangle\langle\phi_0|)^{\otimes N}$ is symmetric and separable. The corresponding correlation function is given by Eq. (55) for $L = 1$ and can be simplified into

$$\mathcal{C}_{ij}^{\mathrm{ex},+}(\mathbf{k}) = I_{00}(\mathbf{k})\, I_{00}(-\mathbf{k}) = |\mathcal{F}_{\mathbf{k}}[|\phi_0(\mathbf{r})|^2]|^2. \tag{67}$$

The decay rates (65) and dipole-dipole shifts (66) read in this case

$$\gamma_{ij} = \iint_{\mathbb{R}^3\times\mathbb{R}^3} \gamma^{\mathrm{cl}}(\mathbf{r}-\mathbf{r}')\, |\phi_0(\mathbf{r})|^2\, |\phi_0(\mathbf{r}')|^2\, d\mathbf{r}\, d\mathbf{r}', \tag{68}$$

$$\Delta_{ij} = \iint_{\mathbb{R}^3\times\mathbb{R}^3} \Delta^{\mathrm{cl}}(\mathbf{r}-\mathbf{r}')\, |\phi_0(\mathbf{r})|^2\, |\phi_0(\mathbf{r}')|^2\, d\mathbf{r}\, d\mathbf{r}'. \tag{69}$$

V. DECAY RATES AND DIPOLE-DIPOLE SHIFTS FOR PARTICULAR MOTIONAL STATES

In this section, we determine *explicit* expressions for the decay rates γ_{ij} and the dipole-dipole shifts Δ_{ij} for different motional states of particular interest. We also discuss the effects of quantum statistics by considering both cases of distinguishable and indistinguishable atoms. For calculation purposes, it is convenient to work in the coordinate system $Ox'y'z'$ as depicted in Fig. 3 with the z' axis along the vector $\mathbf{r}'_{ij} \equiv \mathbf{r}_{ij}$ connecting the atoms i and j, so that $\mathbf{k}'_0\cdot\mathbf{r}'_{ij} = k_0 r_{ij}\cos\theta'$. This coordinate system results from a clockwise rotation of $Oxyz$ by an angle α_{ij} around the y axis.

A. Gaussian states

Gaussian wave packets are of particular importance because they describe a broad class of states, such as the ground state of atoms trapped in harmonic potential, realized, e.g., in a noninteracting Bose-Einstein condensate at zero temperature, but also nonclassical states such as squeezed vibrational states of ions in harmonic trap [73]. We consider N single-atom

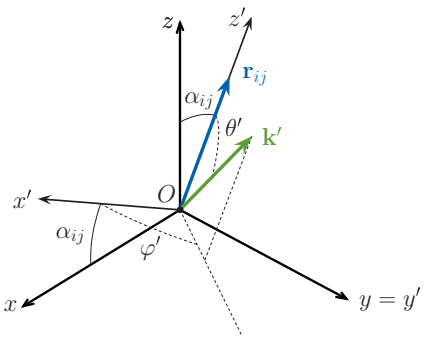

FIG. 3. Coordinate system $Oxyz$ where the z direction corresponds to the quantization axis. The dipole moment for a π transition is $\mathbf{d}_{\pi} = d_0\,\mathbf{e}_z$ with $d_0 \in \mathbb{R}$, and for a $\sigma^{\pm}$ transition is $\mathbf{d}_{\sigma^{\pm}} = d_{\mp}\,\boldsymbol{\varepsilon}_{\mp}$ with $d_{\mp} \in \mathbb{C}$. The vector $\mathbf{r}_{ij}$ connecting the atoms i and j lies in the plane $y = 0$ and forms an angle α_{ij} with the z axis. The primed coordinate system $Ox'y'z'$, equipped with spherical coordinates (k',θ',φ'), is chosen so that $\mathbf{r}'_{ij} \equiv \mathbf{r}_{ij}$ lies along the z' axis in order to facilitate the calculation of the correlation functions.

Gaussian wave packets

$$\phi_j(\mathbf{r}') \equiv \langle \mathbf{r}'|\phi_j\rangle = \prod_{u=x',y',z'} \sqrt{\frac{1}{\sqrt{2\pi}\sigma_u}}\, e^{-(u-u_j)^2/4\sigma_u^2} \tag{70}$$

for $j = 1,\ldots,N$. The wave packets are centered around arbitrary positions $\mathbf{r}'_j = (x'_j, y'_j, z'_j)$ with widths $\sigma_{x'}$, $\sigma_{y'}$, and $\sigma_{z'}$ corresponding to the standard deviations along the three spatial directions, taken equal for all atoms. These states can be seen as the ground states of 3D-harmonically trapped atoms, with $\mathbf{r}'_j$ the position of the center of the trap, $\Omega_u = \hbar/2M\sigma_u^2$ its frequency along the u direction ($u = x', y', z'$), and M the atomic mass. Plugging Eq. (70) into (56), we get for the overlap integral between any two Gaussian states $|\phi_i\rangle$ and $|\phi_j\rangle$

$$I_{ij}(\mathbf{k}) = \prod_{u=x',y',z'} e^{-k_u[k_u\sigma_u^2 - i(u_i+u_j)]/2}\, e^{-(u_i-u_j)^2/8\sigma_u^2}. \tag{71}$$

For simplicity, we now consider $\sigma_{x'} \to 0$ and $\sigma_{y'} \to 0$, so that the atomic motion is only quantized along the z' direction, hence along $\mathbf{r}'_{ij} = (0,0,z'_{ij})$. This is the most interesting case of quantization along only one direction as it allows for the spatial overlap of atomic wave packets. This choice of coordinate system can always be made for $N = 2$ atoms, and the results that we obtain can be transposed to more than two atoms as long as the atoms are aligned along the z' direction. From now on, we denote by $\ell_0 \equiv \sigma_{z'}$ the standard deviation of the Gaussian wave packet along this direction.

1. Distinguishable atoms

For two distinguishable atoms i and j in the states $|\phi_i\rangle$ and $|\phi_j\rangle$, respectively, Eq. (71) yields for the correlation function (55)

$$\begin{aligned}\mathcal{C}_{ij}^{\mathrm{ex,sep}}(\mathbf{k}') &= I_{ii}(\mathbf{k}')\, I_{jj}(-\mathbf{k}') \\ &= e^{-(k'\ell_0\cos\theta')^2} e^{ik'r_{ij}\cos\theta'}.\end{aligned} \tag{72}$$

In the limit of tight confinement, $\ell_0 \to 0$, atoms are well localized and the correlation function reduces to its classical expression $e^{i\mathbf{k}'\cdot\mathbf{r}'_{ij}}$. For any other value of ℓ_0, the decay rates (29) resulting from the correlation function (72) are obtained from the angular integral

$$\gamma_{ij}^{\mathrm{sep}} = \frac{3\gamma_0}{8\pi}\int \sum_{\boldsymbol{\varepsilon}'} |\boldsymbol{\varepsilon}'_{\mathbf{k}'_0}\cdot\mathbf{e}'_{\mathbf{d}'}|^2 e^{-(k_0\ell_0\cos\theta')^2} e^{ik_0 r_{ij}\cos\theta'} d\Omega', \tag{73}$$

with $d\Omega' = \sin\theta' d\theta' d\varphi'$ and where the sum over the polarizations yields a factor $\sum_{\boldsymbol{\varepsilon}'} |\boldsymbol{\varepsilon}'_{\mathbf{k}'_0}\cdot\mathbf{e}'_{\mathbf{d}'}|^2 = 1 - \mu_{ij}$ with

$$\mu_{ij} = (\cos\varphi'\sin\alpha_{ij}\sin\theta' + \cos\alpha_{ij}\cos\theta')^2 \tag{74}$$

for a π transition and

$$\mu_{ij} = \frac{(\cos\theta'\sin\alpha_{ij} - \cos\alpha_{ij}\cos\varphi'\sin\theta')^2 - \sin^2\theta'\sin^2\varphi'}{2} \tag{75}$$

for a $\sigma^{\pm}$ transition. The integral can be evaluated analytically and provides us with the closed formula

$$\gamma_{ij}^{\mathrm{sep}}(\mathbf{r}_{ij},\ell_0) = \frac{3\gamma_0}{16\eta_0^5}\left(\frac{\sqrt{\pi}}{6} e^{-\frac{\xi_{ij}^2}{4\eta_0^2}}\left[16\eta_0^4 - q_{ij}\left(4\eta_0^4 + 3\xi_{ij}^2 - 6\eta_0^2\right)\right]\mathrm{Re}\left\{\mathrm{erf}\left(\eta_0 + \frac{i\xi_{ij}}{2\eta_0}\right)\right\} - q_{ij}\eta_0 e^{-\eta_0^2}\left[2\eta_0^2\cos\xi_{ij} - \xi_{ij}\sin\xi_{ij}\right]\right), \tag{76}$$

where $\mathrm{erf}(z) = \frac{2}{\sqrt{\pi}}\int_0^z e^{-t^2}dt$ is the error function, q_{ij} is the angular factor given by Eq. (33) for a π transition and by Eq. (34) for a $\sigma^{\pm}$ transition, and

$$\xi_{ij} = k_0 r_{ij} = 2\pi\frac{r_{ij}}{\lambda_0}, \quad \eta_0 = k_0\ell_0 = 2\pi\frac{\ell_0}{\lambda_0}. \tag{77}$$

The parameter ξ_{ij} quantifies the significance of atomic cooperative processes. The Lamb-Dicke parameter η_0 is a measure of the recoil experienced by an atom after emission (or absorption) of a photon of wavelength λ_0. Finally, the ratio $\eta_0/\xi_{ij} = \ell_0/r_{ij}$ is a quantifier of the overlap between atomic wave packets (see Fig. 4). Equation (76) is remarkable in that it is valid for any values of both ξ_{ij} and η_0. It provides an accurate description of the combined effects of indeterminacy in atomic positions and recoil on the dissipative dynamics of atoms for any possible realizations of the three characteristic lengths r_{ij}, ℓ_0 and λ_0. In particular, it allows for a full description of recoil effects beyond the Lamb-Dicke regime, i.e., when $\eta_0 \gtrsim 1$. Table I summarizes several regimes that our theory covers as defined through the comparison of the adimensional parameters ξ_{ij} and η_0.

Let us consider two important limiting cases : (I) when the distance between any two atoms is much larger than λ_0 ($\xi_{ij} \gg 1$: no cooperative effects in the case of classical positions), and (II) when the distance between any two atoms is much smaller than λ_0 ($\xi_{ij} \ll 1$: superradiant regime). In the regime I, Eq. (76) reduces to

$$\gamma_{ij}^{\mathrm{sep}} \underset{\xi_{ij}\gg 1}{\simeq} \frac{3\gamma_0}{2}\, p_{ij}\, \frac{\sin\xi_{ij}}{\xi_{ij}}\, e^{-\eta_0^2}, \tag{78}$$

with p_{ij} the angular factor given by Eq. (33) for a π transition and by Eq. (34) for a $\sigma^{\pm}$ transition. This result differs by a factor $e^{-\eta_0^2}$ from the classical result that is obtained for atoms at

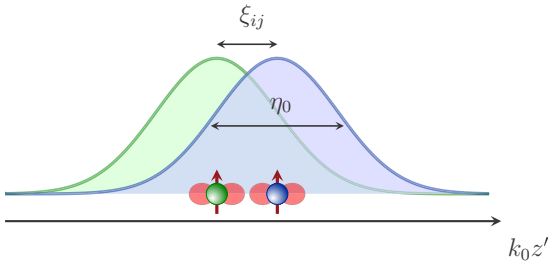

FIG. 4. Schematic view of two atoms separated by a distance r_{ij} and whose positions are described by Gaussian wave packets of width ℓ_0. The dipole moments and dipole radiation patterns are illustrated in red and correspond to a π transition with $\alpha_{ij} = \pi/2$.

TABLE I. Regimes and relevant phenomena related to the different ranges of the adimensional parameters $\xi_{ij} = k_0 r_{ij}$ and $\eta_0 = k_0 \ell_0$. Recoil effects result from photon emission processes and are significant when $\eta_0 \gg 1$. Cooperative effects reflect the fact that the atoms do not behave as independent emitters when $\xi_{ij} \ll 1$ (provided η_0 is not too large; see Fig. 6). Indistinguishability becomes significant as soon as the wave packets overlap (i.e., when $\xi_{ij} \lesssim \eta_0$).

Regime	Relevant phenomena
$1 \lesssim \eta_0 \ll \xi_{ij}$	Recoil effects
$\eta_0 \lesssim \xi_{ij} \ll 1$	Cooperative effects
$1 \ll \xi_{ij} \lesssim \eta_0$	Indistinguishability, recoil effects
$\xi_{ij} \ll 1 \lesssim \eta_0$	Cooperative effects, recoil effects, indistinguishability
$\xi_{ij} \lesssim \eta_0 \ll 1$	Cooperative effects, indistinguishability

fixed positions [i.e., the radiative term of Eq. (32)]. This factor arises from the quantization of the atomic motion and can be interpreted as a reduction of phase coherence in the cooperative emission due to the uncertainty in the atomic positions. It is reminiscent of the Debye-Waller factor $\exp(-k_B T k_0^2/3M\Omega^2)$ typical for neutron scattering, where the position of the atoms is smeared out due to their thermal motion [35] (here T is the temperature, k_B the Boltzmann constant, M the atomic mass, Ω the atomic oscillation frequency, and k_0 the neutron wave number). In the opposite regime ($\xi_{ij} \ll 1$) and for any Lamb-Dicke parameter η_0, Eq. (76) reduces to

$$\gamma_{ij}^{\rm sep} \underset{\xi_{ij}\ll 1}{\simeq} \gamma_0 \left[\sqrt{\pi}\, \mathrm{erf}(\eta_0) \frac{(8-2q_{ij})\eta_0^2 + 3q_{ij}}{16\eta_0^3} - \frac{3q_{ij}\, e^{-\eta_0^2}}{8\eta_0^2} \right]. \tag{79}$$

In particular, in the Lamb-Dicke regime ($\eta_0 \ll 1$), the decay rates decrease with η_0 as

$$\gamma_{ij}^{\rm sep} \underset{\eta_0\ll 1}{\simeq} \gamma_0 \left(1 - \frac{5+q_{ij}}{15}\eta_0^2 \right), \tag{80}$$

while, for large values of η_0, we have

$$\gamma_{ij}^{\rm sep} \underset{\eta_0\gg 1}{\simeq} \gamma_0 \frac{\sqrt{\pi}(4-q_{ij})}{8\eta_0}. \tag{81}$$

We now turn to the calculations of the dipole-dipole shifts. Equation (57) yields for the inverse Fourier transform of (72)

$$\mathcal{F}_{\mathbf{r}'}^{-1}\left[\mathcal{C}_{ij}^{\rm ex,sep}(\mathbf{k}')\right] = \frac{e^{-(z'+z'_{ij})^2/4\ell_0^2}}{2\sqrt{\pi}\,\ell_0}\delta(x')\delta(y'), \tag{82}$$

so that Eq. (52) yields

$$\Delta_{ij}^{\rm sep}(\mathbf{r}_{ij},\ell_0) = \int_{-\infty}^{+\infty} e^{-(z'+z'_{ij})^2/4\ell_0^2}\, \Delta^{\rm cl}(0,0,z')\, \frac{dz'}{2\sqrt{\pi}\,\ell_0}, \tag{83}$$

with $\Delta^{\rm cl}$ given by Eq. (51). Equation (83) depends parametrically on the vector $\mathbf{r}'_{ij} = (0,0,z'_{ij})$ connecting the center of the two Gaussian wave packets. The integral diverges unless a cutoff ϵ is introduced in order to remove the small values of z' around $z' = 0$. Therefore, we introduce the regularized

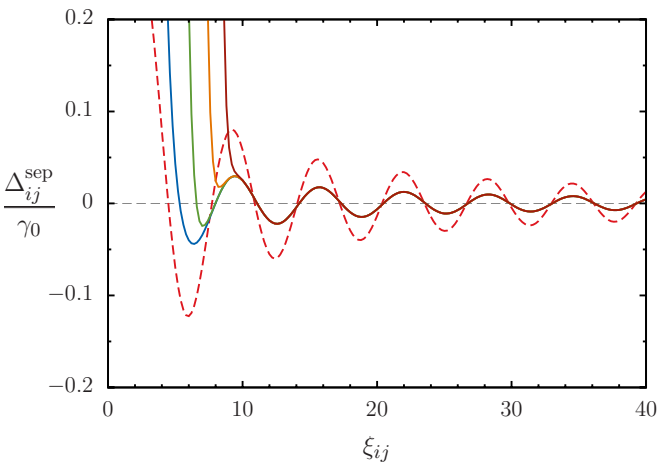

FIG. 5. Regularized dipole-dipole shifts $\Delta_{ij}^{\rm sep}$ as a function of $\xi_{ij} = k_0 r_{ij}$ for atoms in Gaussian states (70) with a Lamb-Dicke parameter $\eta_0 = 1$ and different cutoffs (solid lines from left to right): $k_0\epsilon = 10^{-1}$ (blue curve), $k_0\epsilon = 10^{-2}$ (green curve), $k_0\epsilon = 10^{-3}$ (orange curve), and $k_0\epsilon = 10^{-4}$ (dark red curve). The red dashed curve corresponds to the classical dipole-dipole shift $\Delta^{\rm cl}$ given by Eq. (51). The plots shown are for a π transition with $\alpha_{ij} = \pi/2$.

dipole-dipole shifts

$$\Delta_{ij}^{\rm sep}(\mathbf{r}_{ij},\ell_0,\epsilon) = \left[\int_{-\infty}^{-\epsilon} + \int_{\epsilon}^{+\infty}\right] e^{-(z'+z'_{ij})^2/4\ell_0^2} \times \Delta^{\rm cl}(0,0,z')\, \frac{dz'}{2\sqrt{\pi}\,\ell_0}. \tag{84}$$

In Fig. 5, we show the result of a numerical integration of (84) as a function of ξ_{ij} for different cutoffs ϵ. For $\xi_{ij} \gtrsim 10$, all curves are seen to collapse to a single curve displaying similar oscillations as the classical dipole-dipole shift but with a reduced amplitude (depending on the Lamb-Dicke parameter). The chosen cutoffs have no influence in this parameter range. For $\xi_{ij} \lesssim 10$, the curves corresponding to different cutoffs start to differ. The ones with smaller values of ϵ diverge more rapidly as ξ_{ij} decreases. However, the cutoff cannot be arbitrary small since atoms are not pointlike particles but have a finite spatial extent of the order of the Bohr radius a_0. For frequencies in the optical domain, this leads to the condition $k_0\epsilon > k_0 a_0 \sim 10^{-3}$.

2. *Indistinguishable atoms*

The motional correlation function for indistinguishable atoms in single-atom Gaussian states [see Eq. (70)] is obtained by inserting (71) into (64). The decay rates (29) and dipole-dipole shifts (52) for indistinguishable atoms are thus given by

$$\gamma_{ij}^{\pm}(\{\mathbf{r}_{ij}\},\ell_0) = \sum_{\pi,\pi'} w^{\pi\pi',\pm}\, \gamma_{ij}^{\rm sep}\left(\bar{\mathbf{r}}_{ij}^{\pi\pi'},\ell_0\right), \tag{85}$$

$$\Delta_{ij}^{\pm}(\{\mathbf{r}_{ij}\},\ell_0) = \sum_{\pi,\pi'} w^{\pi\pi',\pm}\, \Delta_{ij}^{\rm sep}\left(\bar{\mathbf{r}}_{ij}^{\pi\pi'},\ell_0\right), \tag{86}$$

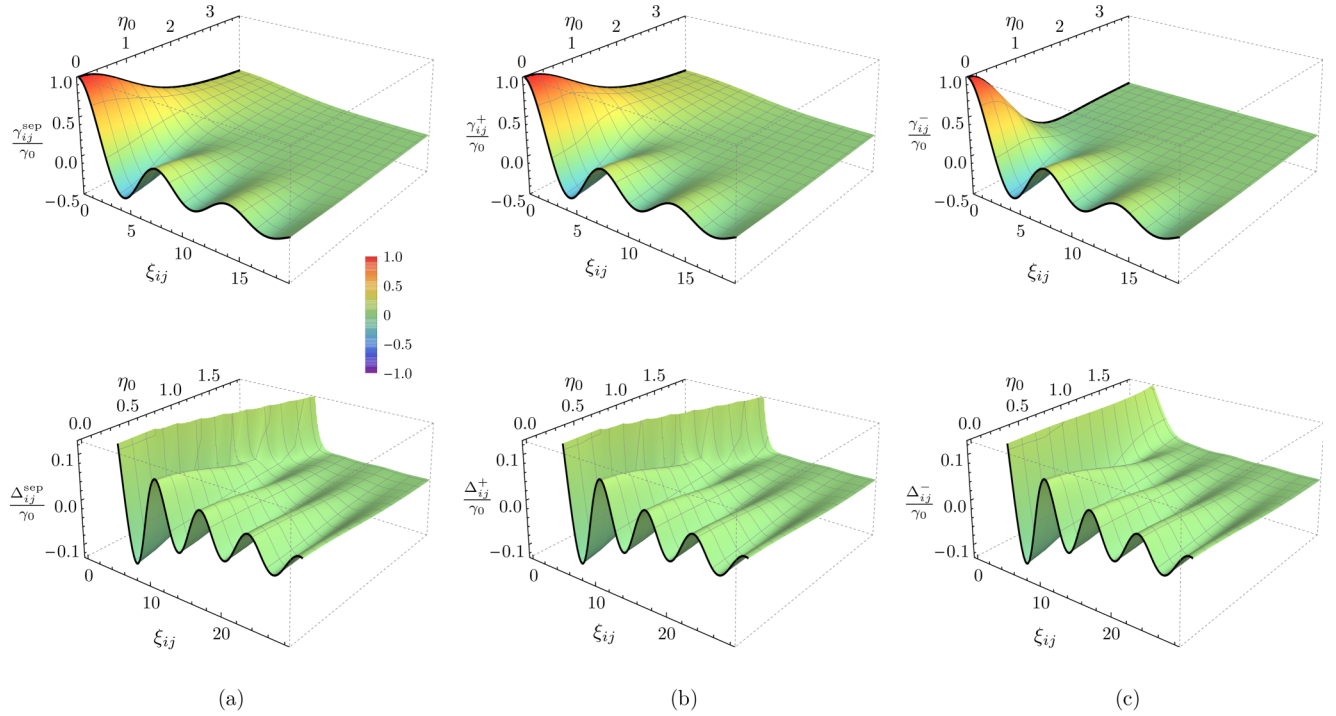

FIG. 6. Off-diagonal decay rates (top) and regularized dipole-dipole shifts (bottom) for the configuration illustrated in Fig. 4 as a function of $\xi_{ij} = k_0 r_{ij}$ and $\eta_0 = k_0 \ell_0$ for (a) distinguishable atoms [Eq. (76) and (84)] and (b), (c) indistinguishable atoms [Eq. (85) and (86) for $N = 2$]. The plots shown are for a π transition with $\alpha_{ij} = \pi/2$ and a cutoff $k_0\epsilon = 0.01$. The black solid curves at the front of each plot (for $\eta_0 = 0$) are the classical decay rate (32) and dipole-dipole shift (51). The black solid curves on the left of each plot of the decay rates (for $\xi_{ij} = 0$) correspond, in the cases (a) and (b), to Eq. (79).

with

$$w^{\pi\pi',\pm} = \frac{s_\pm^{\pi} s_\pm^{\pi'} \prod_{n=1}^{N} e^{-\frac{z'^2_{\pi(n)\pi'(n)}}{8\ell_0^2}}}{\sum_{\tilde\pi,\tilde\pi'} s_\pm^{\tilde\pi} s_\pm^{\tilde\pi'} \prod_{n=1}^{N} e^{-\frac{z'^2_{\tilde\pi(n)\tilde\pi'(n)}}{8\ell_0^2}}}, \tag{87}$$

where $\gamma_{ij}^{\rm sep}$ and $\Delta_{ij}^{\rm sep}$ are given by Eqs. (76) and (84), respectively, and

$$\bar{\mathbf{r}}_{ij}^{\pi\pi'} = \frac{1}{2}(\mathbf{r}_{\pi(i)\pi(j)} + \mathbf{r}_{\pi'(i)\pi'(j)}). \tag{88}$$

Equations (85) and (86) now depend on all $\mathbf{r}_{ij}$, but are equal for all i and j as a consequence of indistinguishability, as discussed in the previous section.

Figure 6 displays the decay rates and regularized dipole-dipole shifts as a function of ξ_{ij} and η_0, both for (a) distinguishable and (b),(c) indistinguishable atoms (corresponding to symmetric and antisymmetric wave functions, respectively). The decay rates $\gamma_{ij}^{\rm sep}$ and $\gamma_{ij}^{\pm}$ are those given in Eqs. (76) and (85), while the dipole-dipole shifts $\Delta_{ij}^{\rm sep}$ and $\Delta_{ij}^{\pm}$ are those given in Eqs. (84) and (86). In the Lamb-Dicke regime ($\eta_0 \ll 1$), the quantum fluctuations of the atomic positions are small and the decay rates and dipole-dipole shifts only slightly depart from their classical values, Eqs. (32) and (51). Beyond the Lamb-Dicke regime ($\eta_0 \gtrsim 1$), the decay rates and dipole-dipole shifts still display oscillations as a function of ξ_{ij} but with a reduced amplitude. This reduction in amplitude is more and more pronounced as η_0 increases. Physically, this can be understood as the result of an average over the atomic positions at the scale of the atomic wave packets of the corresponding oscillating classical quantities [see Eqs. (35) and (52)]. For small interatomic distances in comparison to the wave packets extension ($\xi_{ij} \lesssim \eta_0$), the symmetry of the wave function has major effects on how fast the amplitude decreases with η_0. It is seen to decrease much faster for the antisymmetric wave function than for the symmetric one [see (b) and (c) in the middle panel]. Symmetric and separable wave functions yield very close results because their two-atom reduced density matrices ρ_{ij}^{+} and $\rho_{ij}^{\rm sep}$ are very close. In particular, when $\xi_{ij} \to 0$, we have $\rho_{ij}^{+} \to \rho_{ij}^{\rm sep}$ and $\gamma_{ij}^{+} \to \gamma_{ij}^{\rm sep}$ with $\gamma_{ij}^{\rm sep}$ given by Eq. (79). On the contrary, the two-atom reduced density matrix ρ_{ij}^{-} differs significantly because of the Pauli exclusion principle. When the overlap between atomic wave packets becomes negligible ($\xi_{ij} \gg \eta_0$), the decay rates and the dipole-dipole shifts are approximately equal for the symmetric, antisymmetric, and separable wave functions, showing that atoms can be treated as distinguishable particles in this regime.

B. Harmonic oscillator eigenstates

We now consider as single-atom motional states the vibrational states of harmonically trapped atoms centered around the positions $\mathbf{r}'_j$ ($j = 1, \ldots, N$), hereafter referred as Fock states. We denote them by $|\phi_{(n,\mathbf{r}'_j)}\rangle$ where $n = 0, 1, \ldots$ stands for the number of vibrational excitations. Gaussian states are a particular case ($n = 0$) of this more general class of states. As

previously, atoms are taken to be aligned along the z' direction and their motion is quantized only along this direction.

In the position representation, the single-atom motional Fock states $|\phi_{(n,\mathbf{r}'_j)}\rangle$ with typical size ℓ_0 along z' are given by

$$\phi_{(n,\mathbf{r}'_j)}(\mathbf{r}') = \frac{e^{-(z'-z'_j)^2/4\ell_0^2}}{(2^n n!)^{\frac{1}{2}}\left(2\pi\ell_0^2\right)^{\frac{1}{4}}} H_n\left(\frac{z'-z'_j}{\sqrt{2}\ell_0}\right)\delta(x'_j)\delta(y'_j), \quad (89)$$

where $H_n(z')$ is the Hermite polynomial of order n. The overlap integral (56) between two Fock states at the same position $\mathbf{r}'$ reads [74]

$$I_{(n_i,\mathbf{r}')(n_j,\mathbf{r}')}(\mathbf{k}') = e^{i\mathbf{k}'\cdot\mathbf{r}'}\, e^{-k_{z'}'^2\ell_0^2/2} \times \sqrt{\frac{n_<!}{(n_<+\Delta n)!}}\,(ik'_{z'}\ell_0)^{\Delta n}\, L_{n_<}^{\Delta n}\left(k_{z'}'^2\ell_0^2\right), \quad (90)$$

where L_n^α are the generalized Laguerre polynomials of degree n, $\Delta n = |n_i - n_j|$ and $n_< = \min\{n_i, n_j\}$.

1. Distinguishable atoms

When atom i is in the state $|\phi_{(n_i,\mathbf{r}'_i)}\rangle$ and atom j in the state $|\phi_{(n_j,\mathbf{r}'_j)}\rangle$, according to Eq. (90), the correlation function (55) reads

$$\mathcal{C}_{ij}^{\mathrm{ex,sep}}(\mathbf{k}') = I_{(n_i,\mathbf{r}'_i)(n_i,\mathbf{r}'_i)}(\mathbf{k}')\, I_{(n_j,\mathbf{r}'_j)(n_j,\mathbf{r}'_j)}(-\mathbf{k}') = e^{i\mathbf{k}'\cdot\mathbf{r}'_{ij}}\, e^{-k_{z'}'^2\ell_0^2}\, L_{n_i}^0\left(k_{z'}'^2\ell_0^2\right) L_{n_j}^0\left(k_{z'}'^2\ell_0^2\right). \quad (91)$$

The decay rates of distinguishable atoms with Fock states at arbitrary positions can be obtained by inserting Eq. (91) into Eq. (29) and performing the angular integration. Simple analytical expressions can be obtained in the limit $\xi_{ij} \to 0$ (superradiant regime). To this end, we first express the product of Laguerre polynomials as a linear combination of these same polynomials,

$$L_{n_i}^0(x) L_{n_j}^0(x) = \sum_{\ell=|n_i-n_j|}^{n_i+n_j} c_{n_i,n_j,\ell}\, L_\ell^0(x), \quad (92)$$

with

$$c_{n_i,n_j,\ell} = \left(-\frac{1}{2}\right)^p \sum_n \frac{2^{2n}(n_i+n_j-n)!}{(n_i-n)!(n_j-n)!(2n-p)!(p-n)!}, \quad (93)$$

where $p = n_i + n_j - \ell$ and the sum over n runs over all integers such that the arguments of the factorials are positive [75]. By plugging $\mathcal{C}_{ij}^{\mathrm{ex,sep}}(\mathbf{k}'_0)$ with $e^{i\mathbf{k}'_0\cdot\mathbf{r}'_{ij}} \approx 1$ into Eq. (29) and performing the integration over all directions, we get

$$\gamma_{ij}^{\mathrm{sep}}(n_i,n_j,\ell_0) \underset{\xi_{ij}\ll 1}{\simeq} \frac{\gamma_0}{4}\sum_{\ell=|n_i-n_j|}^{n_i+n_j} c_{n_i,n_j,\ell}\left[q_{ij}\ {}_2F_2\left(\frac{3}{2},\ell+1;1,\frac{5}{2};-\eta_0^2\right) + (4-q_{ij})\ {}_2F_2\left(\frac{1}{2},\ell+1;1,\frac{3}{2};-\eta_0^2\right)\right], \quad (94)$$

with q_{ij} given by Eq. (33) for π transition and by Eq. (34) for $\sigma^\pm$ transition and ${}_pF_q(\mathbf{a};\mathbf{b};z)$ the generalized hypergeometric series [76,77]. The decay rates (94) for atoms in the same Fock state are shown in Fig. 7 as a function of the Lamb-Dicke parameter for a π transition with $\alpha_{ij} = \pi/2$ and for different excitation numbers $n = n_i = n_j$. At fixed Lamb-Dicke parameter, the decay rates are smaller as the excitation number increases. For large Lamb-Dicke parameters, they decrease like a power law, as can be seen from the inset. Some oscillations are present for excitation numbers $n > 0$, which we attribute to oscillations (in momentum space) of the motional wave packets.

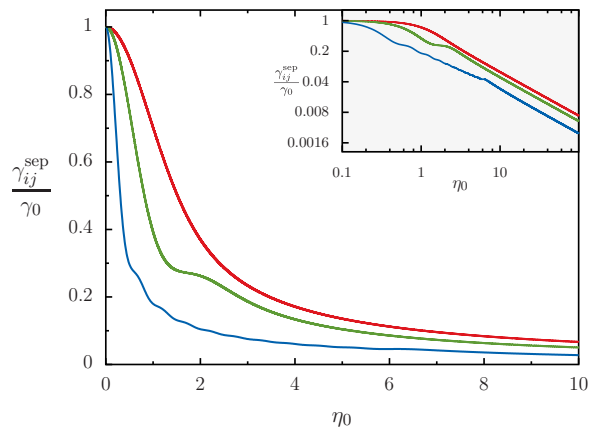

FIG. 7. Decay rates in the superradiant regime in units of γ_0 as a function of the Lamb-Dicke parameter η_0 when atoms i and j are initially in the same motional Fock state $|\phi_{(n,\mathbf{0})}\rangle$ centered around the origin with (from right to left) $n = 0$ (ground state, red curve), $n = 1$ (green curve), and $n = 10$ (blue curve). Inset: same figure in log-log scale showing the power-law decrease of $\gamma_{ij}^{\mathrm{sep}}$ as $1/\eta_0$. The plots shown are for a π transition with $\alpha_{ij} = \pi/2$.

2. Indistinguishable atoms

For indistinguishable atoms in Fock states, the correlation function is given by Eq. (64). The decay rates can be evaluated for arbitrary positions and Lamb-Dicke parameter by inserting (64) into (29). In the limit $\xi_{ij} \to 0$ and for different excitation numbers, the vibrational states are orthogonal and the decay rates can be obtained from

$$\gamma_{ij}^{\pm}(\{n_i\},\ell_0) \underset{\xi_{ij}\ll 1}{\simeq} \frac{1}{N!}\sum_{\pi,\pi'} s_\pm^\pi s_\pm^{\pi'}\, \sigma_{ij}^{\pi,\pi'} \times \int \sum_{\boldsymbol{\varepsilon}} \gamma_{\mathbf{k}_0\boldsymbol{\varepsilon}}^{\mathrm{em}}\, I_{\pi(i)\pi'(i)}(\mathbf{k}_0)\, I_{\pi(j)\pi'(j)}(-\mathbf{k}_0)\,\frac{d\Omega}{(2\pi)^2}, \quad (95)$$

with $\gamma_{\mathbf{k}_0\boldsymbol{\varepsilon}}^{\mathrm{em}}$ and $I_{\alpha\beta}(\mathbf{k}_0)$ given by Eqs. (30) and (90) and

$$\sigma_{ij}^{\pi,\pi'} = \prod_{\substack{n=1\\ n\neq i,j}}^{N} \delta_{\pi(n)\pi'(n)}, \quad (96)$$

where $\delta_{\pi(n)\pi'(n)}$ is the Kronecker symbol. For equal excitation numbers, the symmetric motional state ρ_{ij}^{+} becomes separable in this regime and the symmetric decay rates γ_{ij}^{+} tend to γ_{ij}^{sep} given by Eq. (94).

C. Thermal states in a harmonic trap

We now consider as motional state the thermal state of atoms trapped in a harmonic potential of frequency $\Omega_{z'} = \hbar/2M\ell_0^2$ along the z' direction. In this case, all atoms occupy the same motional mixed state [78]

$$\rho_{(\bar{n},\mathbf{0}')} = \sum_{n=0}^{+\infty} \frac{\bar{n}^n}{(1+\bar{n})^{n+1}} |\phi_{(n,\mathbf{0}')}\rangle\langle\phi_{(n,\mathbf{0}')}| \tag{97}$$

where $\bar{n} = 1/(e^{\hbar\Omega_{z'}/k_BT} - 1)$ is the mean phonon number at temperature T. The overlap

$$I_{(\bar{n},\mathbf{0}')(\bar{n},\mathbf{0}')}(\mathbf{k}') = \left\langle e^{ik'_{z'}\hat{z}'_j}\right\rangle = \text{Tr}\left(e^{ik'_{z'}\hat{z}'_j}\rho_{(\bar{n},\mathbf{0}')}\right) \tag{98}$$

can be evaluated analytically by writing the position operator as $\hat{z}'_j = \ell_0(b_j + b_j^\dagger)$ with b_j and $b_j^\dagger$ the annihilation and creation operators of a motional excitation for atom j. Upon using the identity $\langle \exp[\ell_0(b_j^\dagger + b_j)]\rangle = \exp[\ell_0^2\langle(b_j^\dagger + b_j)^2\rangle]$, where the expectation value is taken in a thermal state [79], we get

$$I_{(\bar{n},\mathbf{0}')(\bar{n},\mathbf{0}')}(\mathbf{k}') = e^{-k_{z'}'^2\ell_0^2(2\bar{n}+1)/2}. \tag{99}$$

The corresponding correlation function (55) reads

$$\mathcal{C}_{ij}^{\text{ex,sep}}(\mathbf{k}') = e^{-k_{z'}'^2\ell_0^2(2\bar{n}+1)}, \tag{100}$$

and is of the same form as for Gaussian states centered around the origin [see Eq. (72)], now with a width $\tilde{\ell}_0 = \ell_0\sqrt{2\bar{n}+1}$ which depends on the temperature through $\bar{n}$. As a consequence, the decay rates and the dipole-dipole shifts for atoms in the same thermal state are given by Eqs. (76) and (84) with η_0 replaced by $\tilde{\eta}_0 = \eta_0\sqrt{2\bar{n}+1}$. The increase in Lamb-Dicke parameter from η_0 to $\tilde{\eta}_0$ comes from the Debye-Waller factor $e^{-k_0^2\langle\hat{z}_j'^2\rangle}$ where $\langle\hat{z}_j'^2\rangle = \ell_0^2(2\bar{n}+1)$ is the mean square displacement of atom j.

VI. CONCLUSIONS

In this work, we derived a general master equation for the internal dynamics of atoms coupled to the electromagnetic field in vacuum, taking into account the quantization of their motion. Our master equation provides an accurate description of recoil effects, even beyond the Lamb-Dicke regime, and applies equally well to distinguishable and indistinguishable atoms. We obtained general expressions for the dipole-dipole shifts and the decay rates, which determine the conservative and dissipative atomic internal dynamics, in terms of their classical expressions and the motional correlation function defined for arbitrary motional states. We showed that the motional state allows one to engineer the dipole-dipole shifts and the decay rates, and can lead to a large modification compared to the classical value. In particular, we obtained analytical expressions for the decay rates for Gaussian states, harmonic oscillator eigenstates, and thermal states, that are relevant in cold atom experiments. In a forthcoming work, we will present a detailed study of the general solutions of our master equation.

ACKNOWLEDGMENTS

F.D. would like to thank the F.R.S.-FNRS for financial support. F.D. is supported by the Fonds de la Recherche Scientifique-FNRS.

[1] A. Einstein, Verhandlungen der Deutschen Physikalischen Gesellschaft **18**, 318 (1916).
[2] V. Weisskopf and E. Wigner, Z. Phys. **63**, 54 (1930).
[3] E. M. Purcell, H. C. Torrey, and R. V. Pound, Phys. Rev. **69**, 37 (1946).
[4] V. P. Bykov, Sov. Phys. JETP **35**, 269 (1972).
[5] E. Yablonovitch, Phys. Rev. Lett. **58**, 2059 (1987).
[6] S. John, Phys. Rev. Lett. **58**, 2486 (1987).
[7] R. H. Dicke, Phys. Rev. **93**, 99 (1954).
[8] R. Bonifacio, P. Schwendiman, and F. Haake, Phys. Rev. A **4**, 302 (1971).
[9] R. Bonifacio, P. Schwendiman, and F. Haake, Phys. Rev. A **4**, 854 (1971).
[10] L. M. Narducci, C. A. Coulter, and C. M. Bowden, Phys. Rev. A **9**, 829 (1974).
[11] R. J. Glauber and F. Haake, Phys. Rev. A **13**, 357 (1976).
[12] M. Gross and S. Haroche, Phys. Rep. **93**, 301 (1982).
[13] G. Nienhuis and F. Schuller, J. Phys. B: At. Mol. Phys. **20**, 23 (1987).
[14] R. G. DeVoe and R. G. Brewer, Phys. Rev. Lett. **76**, 2049 (1996).
[15] P. A. Braun, D. Braun, F. Haake, and J. Weber, Eur. Phys. J. D **2**, 165 (1998).
[16] P. A. Braun, D. Braun, and F. Haake, Eur. Phys. J. D **3**, 1 (1998).
[17] Y. N. Chen, C. M. Li, D. S. Chuu, and T. Brandes, New J. Phys. **7**, 172 (2005).
[18] E. Akkermans, A. Gero, and R. Kaiser, Phys. Rev. Lett. **101**, 103602 (2008).
[19] D. Braun, J. Hoffman, and E. Tiesinga, Phys. Rev. A **83**, 062305 (2011).
[20] R. Wiegner, J. von Zanthier, and G. S. Agarwal, Phys. Rev. A **84**, 023805 (2011).
[21] S. Oppel, R. Wiegner, G. S. Agarwal, and J. von Zanthier, Phys. Rev. Lett. **113**, 263606 (2014).
[22] R. Wiegner, S. Oppel, D. Bhatti, J. von Zanthier, and G. S. Agarwal, Phys. Rev. A **92**, 033832 (2015).
[23] D. Bhatti, J. von Zanthier, and G. S. Agarwal, Sci. Rep. **5**, 17335 (2015).
[24] S. Inouye, A. P. Chikkatur, D. M. Stamper-Kurn, J. Stenger, D. E. Pritchard, and W. Ketterle, Science **285**, 571 (1999).
[25] B. Coffey and R. Friedberg, Phys. Rev. A **17**, 1033 (1978).
[26] F. Friedberg and S. R. Hartmann, Phys. Rev. A **10**, 1728 (1974).
[27] H. S. Freedhoff, J. Phys. B: At. Mol. Phys. **19**, 3035 (1986).
[28] H. S. Freedhoff, J. Phys. B: At. Mol. Phys. **20**, 285 (1987).
[29] W. Feng, Y. Li, and S.-Y. Zhu, Phys. Rev. A **88**, 033856 (2013).
[30] Th. Richter, J. Phys. B: At. Mol. Opt. Phys. **23**, 4415 (1990).

[31] R. Friedberg, S. R. Hartmann, and J. T. Manassah, Phys. Lett. A **40**, 365 (1972).

[32] T. Bienaimé, N. Piovella, and R. Kaiser, Phys. Rev. Lett. **108**, 123602 (2012).

[33] M. D. Lukin, M. Fleischhauer, R. Cote, L. M. Duan, D. Jaksch, J. I. Cirac, and P. Zoller, Phys. Rev. Lett. **87**, 037901 (2001).

[34] R. M. Sandner, M. Müller, A. J. Daley, and P. Zoller, Phys. Rev. A **84**, 043825 (2011).

[35] P. Debye, Ann. Phys. **348**, 49 (1913).

[36] I. Waller, Z. Phys. A **17**, 398 (1923).

[37] J. I. Cirac and P. Zoller, Phys. Rev. Lett. **74**, 4091 (1995).

[38] K. Mølmer and A. Sørensen, Phys. Rev. Lett. **82**, 1835 (1999).

[39] P. Lodahl, A. Floris van Driel, I. S. Nikolaev, A. Irman, K. Overgaag, D. Vanmaekelbergh, and W. L. Vos, Nature (London) **430**, 654 (2004).

[40] J. Javanainen, J. Opt. Soc. Am. B **5**, 73 (1988).

[41] R. G. Brewer, Phys. Rev. A **52**, 2965 (1995).

[42] A. W. Vogt, J. I. Cirac, and P. Zoller, Phys. Rev. A **53**, 950 (1996).

[43] D. Leibfried, R. Blatt, C. Monroe, and D. Wineland, Rev. Mod. Phys. **75**, 281 (2003).

[44] D. Braun and J. Martin, Phys. Rev. A **77**, 032102 (2008).

[45] H. Pichler, A. J. Daley, and P. Zoller, Phys. Rev. A **82**, 063605 (2010).

[46] J. Cerrillo, A. Retzker, and M. B. Plenio, Phys. Rev. Lett. **104**, 043003 (2010).

[47] J. Yin and J. Javanainen, Phys. Rev. A **51**, 3959 (1995).

[48] B. Dubetsky and P. R. Berman, Phys. Rev. A **53**, 390 (1996).

[49] P. R. Berman, Phys. Rev. A **55**, 4466 (1997).

[50] G. Morigi, J. Eschner, J. I. Cirac, and P. Zoller, Phys. Rev. A **59**, 3797 (1999).

[51] M. J. McDonnell, J. P. Home, D. M. Lucas, G. Imreh, B. C. Keitch, D. J. Szwer, N. R. Thomas, S. C. Webster, D. N. Stacey, and A. M. Steane, Phys. Rev. Lett. **98**, 063603 (2007).

[52] M. Roghani, and H. Helm, Phys. Rev. A **77**, 043418 (2008).

[53] K. Afrousheh, P. Bohlouli-Zanjani, D. Vagale, A. Mugford, M. Fedorov, and J. D. D. Martin, Phys. Rev. Lett. **93**, 233001 (2004).

[54] F. Robicheaux, J. V. Hernández, T. Topçu, and L. D. Noordam, Phys. Rev. A **70**, 042703 (2004).

[55] E. Altiere, D. P. Fahey, M. W. Noel, R. J. Smith, and T. J. Carroll, Phys. Rev. A **84**, 053431 (2011).

[56] J. Pellegrino, R. Bourgain, S. Jennewein, Y. R. P. Sortais, A. Browaeys, S. D. Jenkins, and J. Ruostekoski, Phys. Rev. Lett. **113**, 133602 (2014).

[57] S. Y. Buhmann, *Dispersion Forces*, Springer Tracts In Modern Physics Vol. 248 (Springer, New York, 2012).

[58] E. A. Power and S. Zienau, Philos. Trans. R. Soc. **251**, 427 (1959).

[59] C. Cohen-Tannoudji, J. Dupont-Roc, and G. Grynberg, *Photons et atomes, Introduction à l'électrodynamique quantique* (EDP Sciences, Paris, 1987).

[60] We emphasize the quantum treatment of the atomic motion by writing the center-of-mass position and momentum operators $\hat{\mathbf{r}}$ and $\hat{\mathbf{p}}$, in contrast to the classical center-of-mass position and momentum which are denoted by $\mathbf{r}$ and $\mathbf{p}$, respectively.

[61] H.-P. Breuer and F. Petruccione, *The Theory of Open Quantum Systems* (Oxford University Press, Oxford, 2006).

[62] D. A. Lidar, Z. Bihary, and K. B. Whaley, Chem. Phys. **268**, 35 (2001).

[63] See Supplemental Material at http://link.aps.org/supplemental/10.1103/PhysRevA.93.022124 for technical details about the derivation of our master equation.

[64] This choice is perfectly justified in the optical domain since optical modes of the electromagnetic field in thermal equilibrium at a temperature below 300 K are essentially in the ground state.

[65] C. W. Gardiner and P. Zoller, *Quantum Noise*, 3rd ed. (Springer, Berlin, Heidelberg, New York, 2004).

[66] The RWA is valid as long as the relaxation time of the system, $\tau_R \sim 1/\gamma_0$, is much larger than the typical time scale τ_S of its intrinsic evolution. Here the intrinsic evolution corresponds to the internal dynamics of the atoms; hence $\tau_S \sim 1/\omega_0$. We thus have $\tau_S/\tau_R \sim \gamma_0/\omega_0 \sim \alpha(a_0/\lambda_0)^2$ with α the fine-structure constant, a_0 the Bohr radius, and λ_0 the wavelength of the emitted radiation. In the optical domain, this ratio is much smaller than one and the dipole approximation and RWA are entirely justified.

[67] M. J. Stephen, J. Chem. Phys. **40**, 669 (1964).

[68] G. S. Agarwal, *Quantum Statistical Theories of Spontaneous Emission and Their Relation to Other Approaches*, Springer Tracts In Modern Physics Vol. 70 (Springer, New York, 1974), p. 1.

[69] In this work, we use for the Fourier transform $\mathcal{F}_{\mathbf{k}}[\cdot]$ and its inverse $\mathcal{F}^{-1}_{\mathbf{r}}[\cdot]$ the convention

$$\mathcal{F}_{\mathbf{k}}[f] = \int_{\mathbb{R}^3} e^{-i\mathbf{k}\cdot\mathbf{r}} f(\mathbf{r}) d\mathbf{r}, \quad \mathcal{F}^{-1}_{\mathbf{r}}[g] = \int_{\mathbb{R}^3} e^{i\mathbf{k}\cdot\mathbf{r}} g(\mathbf{k}) \frac{d\mathbf{k}}{(2\pi)^3}.$$

[70] The principal value arising here is a mere consequence of second-order perturbation theory since resonant intermediate transitions must be discarded [71].

[71] M. Donaire, R. Guérout, and A. Lambrecht, Phys. Rev. Lett. **115**, 033201 (2015).

[72] Note that this is a consequence of the second-order perturbative treatment for the atom-field interaction. As van der Waals dipole-dipole interactions between two atoms in the same internal state result from a fourth-order perturbative development, they are not considered in this work.

[73] Z. Heping and L. Fucheng, Chin. Phys. Lett. **12**, 203 (1995).

[74] D. J. Wineland and W. M. Itano, Phys. Rev. A **20**, 1521 (1979).

[75] J. Gillis and G. Weiss, Math. Comp. **14**, 60 (1960).

[76] M. Abramowitz and A. Stegun, *Handbook of Mathematical Functions* (Dover Publications Inc., New York, 1970).

[77] The generalized hypergeometric series is defined by

$${}_pF_q(\mathbf{a};\mathbf{b};z) = \sum_{k=0}^{+\infty} \frac{(a_1)_k \dots (a_p)_k}{(b_1)_k \dots (b_q)_k} \frac{z^k}{k!}$$

with $(\cdot)_k$ the Pochhammer symbol defined as $(a)_0 = 1$ and

$$(a)_k = a(a+1)(a+2)\cdots(a+k-1) = \frac{(a+k-1)!}{(a-1)!}.$$

[78] There is no contradiction with the fact that we consider the e.m. field in vacuum. Indeed, since the motional frequency $\Omega_{z'}$ is much smaller than the field frequencies $\omega \sim \omega_0$ which contribute significantly to the dynamics, the motional and the e.m. field states can be taken respectively thermally excited and in vacuum at the same time.

[79] K. Huang, *Introduction to Statistical Physics* (Taylor and Francis, London, 2001).